

## High spin states in $^{63}\text{Cu}$

B MUKHERJEE<sup>1,2</sup>, S MURALITHAR<sup>1</sup>, R P SINGH<sup>1</sup>, R KUMAR<sup>1</sup>, K RANI<sup>1</sup>,  
S C PANCHOLI<sup>3</sup> and R K BHOWMIK<sup>1</sup>

<sup>1</sup>Nuclear Science Centre, P.B. No. 10502, New Delhi 110 067, India

<sup>2</sup>Jawaharlal Nehru University, New Delhi 110 067, India

<sup>3</sup>Department of Physics and Astrophysics, Delhi University, Delhi 110 007, India

MS received 12 May 2000; revised 24 July 2000

**Abstract.** Excited states of  $^{63}\text{Cu}$  were populated via the  $^{52}\text{Cr} + ^{16}\text{O}$  (65 MeV) reaction using the gamma detector array equipped with charged particle detector array for reaction channel separation. On the basis of  $\gamma$ - $\gamma$  coincidence relations and angular distribution ratios, a level scheme was constructed up to  $E_x = 7$  MeV and  $J^\pi = 23/2^{(+)}$ . The decay scheme deduced was interpreted in terms of shell model calculations, with a restricted basis of the  $f_{5/2}, p_{3/2}, p_{1/2}, g_{9/2}$  orbitals outside a  $^{56}_{28}\text{Ni}$  core.

**Keywords.** Nuclear reaction  $^{52}\text{Cr}(^{16}\text{O}, \alpha p)^{63}\text{Cu}$  at  $E = 65$  MeV; measured  $E_\gamma; I_\gamma; \gamma$ - $\gamma$ -charged particle coincidence;  $^{63}\text{Cu}$  deduced levels;  $J^\pi$ ; DCO ratio; shell-model calculation.

**PACS Nos** 21.10.Hw; 23.20.Lv; 27.50.+e

### 1. Introduction

The mechanism for the generation of high angular momentum states in the restricted valence space around the  $^{56}\text{Ni}$  core poses an interesting physics question. Energetically speaking, the first three shell-model orbitals above the  $N = Z = 28$  closed shell are the negative parity  $p_{3/2}, f_{5/2}$ , and  $p_{1/2}$  orbitals. The generation of higher spin states requires either the breaking of the  $^{56}\text{Ni}$  core and/or excitation into the positive parity  $g_{9/2}$  shell. The identification of this competing mechanism is one of the main motivations for the study of the high spin states in the  $A \sim 60$  region. Such work is also of interest in the light of recent experimental evidence of a near-yrast superdeformed minimum [1–5] and smooth band termination [6,7] at high spins in this region. The low-lying level structure of  $^{63}\text{Cu}$  has been investigated through various light-ion induced experiments [8–12], but the information of high-spin states is limited [13]. Here we present the preliminary results of a near yrast study of an  $fpg$  shell system  $^{63}\text{Cu}$ . In addition to the general interest in the build up of high-spin configurations outlined above, a detailed and careful study of the medium spin, near yrast states in this nucleus is important for reliable assignments of spins and parities to states in superdeformed bands [1,6] in mass region 60. Also, the observation of direct proton decay from excited states in Cu nuclei [14] makes it important to determine

the excitation energies, spins, and parities of levels in this mass region, in order to provide a complete characterization of the proton-decaying states.

## 2. Experimental details

One experiment was performed at the Nuclear Science Centre, New Delhi, using a 65 MeV beam of  $^{16}\text{O}$ , provided by the 15 UD Pelletron facility, incident on a gold-backed natural chromium target. This experiment used a  $1\text{ mg/cm}^2$   $^{52}\text{Cr}$  target evaporated onto a thick  $7.2\text{ mg/cm}^2$  Au backing. Prompt  $\gamma$ -rays were detected using the gamma detector array (GDA) [15] of twelve germanium detectors (HPGe) with BGO Compton suppressors, in coincidence with the evaporated lightly charged particles, which were detected with the  $4\pi$  charged particle detector array (CPDA) [16]. The energy resolutions of the HPGe detectors were 1.5–2.3 keV for the 1.3 MeV  $\gamma$ -rays. The efficiencies were about 25% relative to a standard  $3'' \Phi \times 3''$  NaI detector. The CPDA, consisted of fourteen phoswich  $\Delta E$ - $E$  detectors, which are made of fast-slow plastic scintillators (BC400 and BC444), selected the evaporation channels of the charged particles.

## 3. Data analysis and results

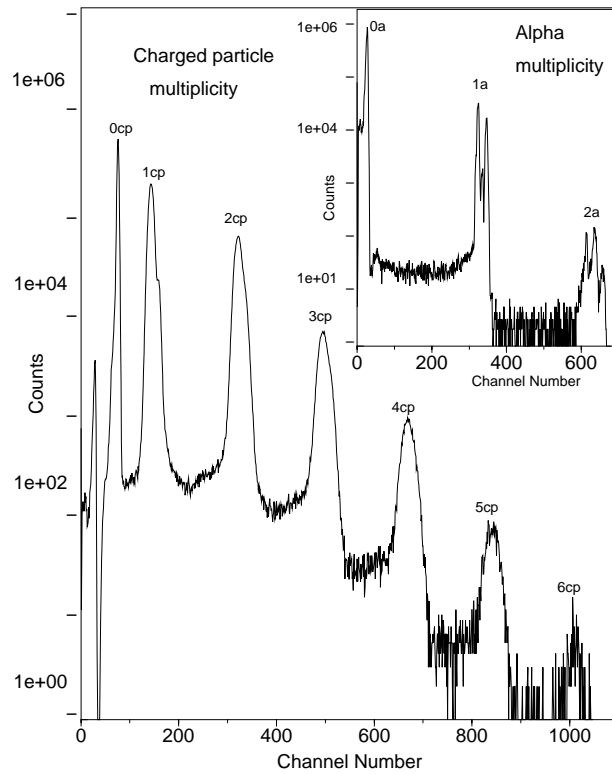
A total of  $9.4 \times 10^7$   $\gamma$ - $\gamma$ -charged particle coincidence events were collected event by event for an offline analysis, from which  $\gamma$ - $\gamma$  matrices were created by applying different gating conditions set on the number of detected protons and/or  $\alpha$  particles. The  $\gamma$ - $\gamma$  coincidence relationship for  $^{63}\text{Cu}$  were derived from a  $4k \times 4k$  matrix gated on the  $1\alpha 1p$  reaction channel.

Figure 1 shows the typical charged particle- and  $\alpha$ - (inset) multiplicity spectrum, which were used finally to gate on the raw  $\gamma$ - $\gamma$  spectrum to identify the  $\gamma$ -rays belonging to different reaction channels. Each sharp peak position marked with number and type of multiplicity clearly gives evidence of the clean separation, and, hence identification of different charged particle reaction channel. A comparison of a typical projected  $\gamma$ -spectrum from the total matrix (where no charged particle condition is used) with that of an  $\alpha p$  gated matrix is shown in figure 2. Panels (a) and (b) in figure 2 present an ungated and  $1\alpha 1p$ -gated  $\gamma$ -ray spectrum, respectively, while panel (c) is the spectrum obtained by putting a gate on 342 keV transition of  $^{63}\text{Cu}$  from the  $\alpha p$  gated matrix. Coincidence, intensity balance, and summed energy relations were inspected to deduce the high spin states. The  $\gamma$ - $\gamma$  spectrum gated by  $1\alpha 1p$  exit channel, in panel (b) of figure 2, has the breakthrough of higher multiplicity reaction channels, in particular, of the  $1\alpha 1p 1n$  channel ( $^{62}\text{Cu}$ ) [17], which is most abundantly produced in this reaction. Therefore, this spectrum shows the  $\gamma$ -rays of  $^{63}\text{Cu}$  as well as of  $^{62}\text{Cu}$  with a high ratio of peak to background and very high purity.

High resolution  $\gamma$ - $\gamma$  coincidence matrix was then incremented from which decay scheme of  $^{63}\text{Cu}$  was constructed. The  $\gamma$ -ray energies and intensities presented in the level scheme (cf. figure 3) are based on the previously mentioned  $1\alpha 1p$  gated  $\gamma$ - $\gamma$  matrix. But for weak transitions and/or doublet structures,  $\gamma$ -gated spectra obtained from total  $\gamma$ - $\gamma$  matrix were considered. Spin and parity assignments were made on the basis of a DCO-type analysis [18] and from the known  $3/2^-$  spin-parity value of the ground state. A separate  $\gamma$ - $\gamma$  coincidence matrix was constructed with events detected in detectors at  $153^\circ$  ( $\theta_1$ ) versus those at  $99^\circ$  ( $\theta_2$ ) detectors. By gating a transition of known multipolarity on each axis of this matrix, a DCO ratio

$$R_{\text{dco}} = \frac{I_{\gamma_1}(\theta_1) \text{ gated by } \gamma_2(\theta_2)}{I_{\gamma_1}(\theta_2) \text{ gated by } \gamma_2(\theta_1)}$$

could be obtained. For an (E2, E2) coincidence,  $R_{\text{dco}}$  was found to be approximately 1.0, while for (E2, E1/M1) pairs,  $R_{\text{dco}} \approx 0.6$ . Definite parities were assigned to the excited states if one of their de-exciting transitions was stretched E2 or mixed M1/E2 transition, while in the case of pure dipole transitions only tentative parities were ascribed. The energies, relative intensities, and DCO ratios of the  $\gamma$ -rays are given in table 1. Intensity values are obtained from the total projected spectrum and are normalized with respect to that of 962 keV  $\gamma$ -ray. The DCO ratios are obtained from the spectra gated by an E2 342 keV transition. The DCO ratios of some of the transitions could not be measured because they were weak in intensity. Hence, no definite conclusion could be drawn about the spin-parity of some levels, which are left vacant in the table. The decay scheme of  $^{63}\text{Cu}$  derived from



**Figure 1.** Typical multiplicity spectrum of evaporated charged particles (either proton or  $\alpha$ ) and  $\alpha$  (inset) detected in the CPDA. Each sharp peak position marked with number and type of multiplicity ('cp' for charged particle and 'a' for  $\alpha$ ) clearly evidences the clean separation and, hence, identification of different charged particle reaction channels.

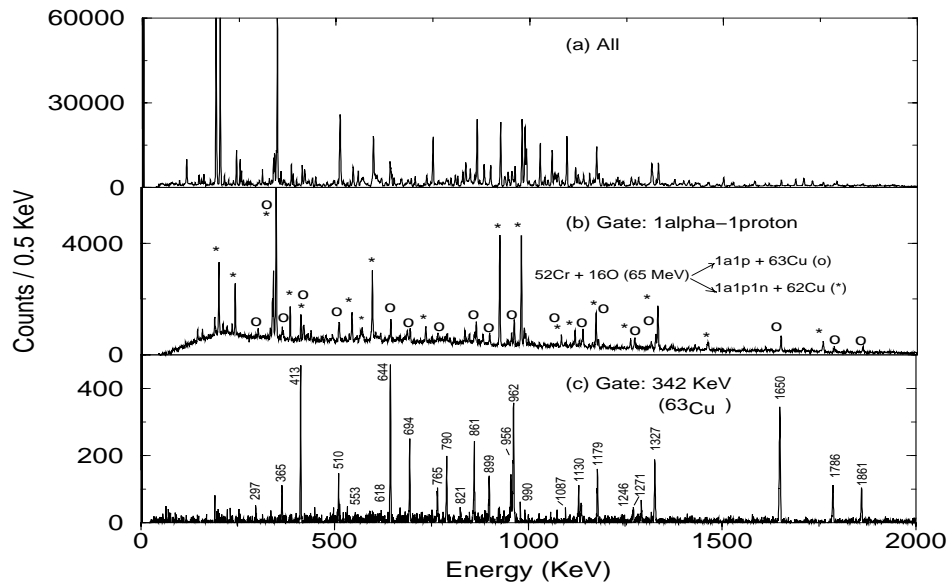


**Figure 2.**  $\gamma$ -ray spectra: (a) with no condition, (b) gated by  $1\alpha 1p$  and (c) gated by  $1\alpha 1p$  and 342 keV transition of  $^{63}\text{Cu}$ .

this work is shown in figure 3. All the transitions marked in the panel (c) of figure 2 are assigned in the level scheme except X-rays and  $\gamma$ -rays from gold backing. This present work confirms almost all the states proposed in the earlier experiments [8–13], most of which had used light-ion induced reactions to populate the nuclei. In addition, a total of eight previously unreported states and 17 new  $\gamma$  transitions (marked by an asterisk in figure 3) have been observed and properly placed in the level scheme, thereby, extending the level scheme of  $^{63}\text{Cu}$  up to an excitation energy of  $\sim 7$  MeV and spin-parity of  $23/2^{+}$ . The energies of newly assigned  $\gamma$ -rays are 297, 368, 406, 510, 526, 553, 618, 668, 790 (doublet), 821, 990, 1087, 1271, 1291, 1543, and 1707 keV. We have observed some of these  $\gamma$  rays linking some of the already established levels, which have resulted in predicting and/or assigning spin parities of the known levels in a more conclusive way. In the gated spectra we could find several other  $\gamma$ -rays, which could not be placed in the level scheme due to lack of proper coincidence relations. The states with tentative spin-parity  $9/2^{+}$ ,  $13/2^{+}$ ,  $17/2^{+}$  and  $19/2^{+}$  at 2505, 4155, 4497 and 6283 keV respectively are confirmed in the present work. Gamma-rays of 406, 821, 990, 1271, 1291 keV transition energies in the data set, depopulating the states at 2912, 5319, 1952, 5769, 2618 keV respectively, had insufficient statistics to extract useful numbers of DCO ratios; they consequently remain unassigned. This does, however, constitute the first observation of these states and their place in the decay scheme is therefore significant. The state  $(23/2^{+})$  at 7073 keV, depopulating via 790 keV transition, is observed to be the highest spin state in the decay scheme.

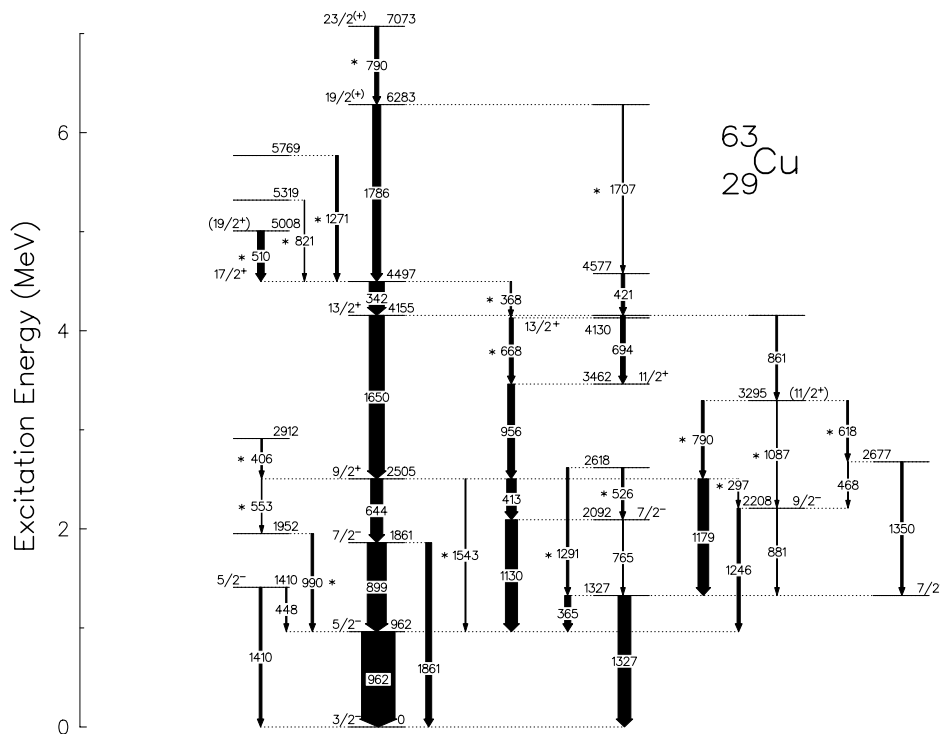


**Figure 3.** Proposed level scheme for  $^{63}\text{Cu}$ . All transitions have satisfied  $\gamma$ - $\gamma$  coincidence conditions, and the width of the arrows corresponds to the relative  $\gamma$ -ray intensities.

#### 4. Shell model comparison and discussion

Shell model calculations have been performed for  $^{63}\text{Cu}$  with a model space basis restricted to the  $f_{5/2}$ ,  $p_{3/2}$ ,  $p_{1/2}$ , and  $g_{9/2}$  orbitals (henceforth called  $fp_g$  shell calculations), using the OXBASH code [19]. The two-body matrix elements were taken from the work of Koops *et al* [20]. The model assumes a closed  $^{56}_{28}\text{Ni}$  core and does not allow for core breaking. For both the protons and neutrons, the single-particle energies of these active orbitals were calculated relative to the lowest  $f_{5/2}$  state, and found to be 1.01 MeV for  $p_{3/2}$ , 2.83 MeV for  $p_{1/2}$ , and 0.68 MeV for  $g_{9/2}$  orbital.

For  $^{63}_{29}\text{Cu}_{34}$ , the  $fp_g$ -shell model space has six valence neutrons and one valence proton in the four active orbitals, and the maximum angular momentum that can be generated is  $(\pi g_{9/2})^1_{9/2^+} \otimes (\nu g_{9/2})^4_{12^+} \otimes (\nu f_{5/2})^2_{4^+} = \frac{41}{2} + \hbar$ . The results of this calculation are compared with the experimental levels in figure 4.

While the calculation has not been used to unambiguously assign spins or parities, it has been useful in inferring probable assignments, or in supporting the validity of claims made from the DCO data or intensities.

First few states with negative parity are well reproduced within 50 keV. Some low-lying states of +ve parity are also well reproduced but the yrast  $17/2^+$  state at 4497 keV and

**Table 1.** Level energies ( $E_x$ ), transition energies ( $E_\gamma$ ), initial ( $I_i^\pi$ ) and final ( $I_f^\pi$ ) spin-parity of the transitions, relative intensities of  $\gamma$ -ray transitions ( $I_\gamma$ ) and DCO ratios ( $R_{\text{dco}}$ ) are shown for  $^{63}\text{Cu}$ , as obtained from the present work. The error in the  $\gamma$ -ray energy is about 0.1 keV. The DCO ratios of some of the transitions could not be measured because of their weak intensities.

$E_x$ (keV)	$E_\gamma$ (keV)	$I_i^\pi$ ( $\hbar$ )	$I_f^\pi$ ( $\hbar$ )	$I_\gamma$ (%)	$R_{\text{dco}}$
962	962	$5/2^-$	$3/2^-$	100	0.55
1327	365	$7/2^-$	$5/2^-$	18	0.73
	1327	$7/2^-$	$3/2^-$	38	1.10
1410	448	$5/2^-$	$5/2^-$	4	
	1410	$5/2^-$	$3/2^-$	10	0.62
1861	899	$7/2^-$	$5/2^-$	8	0.51
	1861	$7/2^-$	$3/2^-$	18	0.94
1952	990			8	
2092	765	$7/2^-$	$7/2^-$	3	
	1130	$7/2^-$	$5/2^-$	37	0.63
2208	881	$9/2^-$	$7/2^-$	3	
	1246	$9/2^-$	$5/2^-$	10	0.98
2505	297	$9/2^+$	$9/2^-$	3	
	413	$9/2^+$	$7/2^-$	28	0.61
	553	$9/2^+$		2	
	644	$9/2^+$	$7/2^-$	36	0.47
	1179	$9/2^+$	$7/2^-$	33	0.67
	1543	$9/2^+$	$5/2^-$	4	
2618	526		$7/2^-$	7	
	1291		$7/2^-$	8	
2677	468		$9/2^-$	3	
	1350		$7/2^-$	8	
2912	406		$9/2^+$	4	
3295	618	$(11/2^+)$		5	
	790	$(11/2^+)$	$9/2^+$	8	
	1087	$(11/2^+)$	$9/2^-$	2	
3462	956	$11/2^+$	$9/2^+$	21	0.55
4130	668	$13/2^+$	$11/2^+$	12	0.74
4155	694	$13/2^+$	$11/2^+$	14	0.43
	861	$13/2^+$	$(11/2^+)$	6	0.41
	1650	$13/2^+$	$9/2^+$	45	1.13
4497	342	$17/2^+$	$13/2^+$	45	1.02
	368	$17/2^+$	$13/2^+$	4	
4577	421		$13/2^+$	10	
5008	510	$(19/2^+)$	$17/2^+$	20	0.49
5319	821		$17/2^+$	2	
5769	1271		$17/2^+$	8	
6283	1707	$19/2^{(+)}$		3	
	1786	$19/2^{(+)}$	$17/2^+$	24	0.62
7073	790	$23/2^{(+)}$	$19/2^{(+)}$	13	1.15

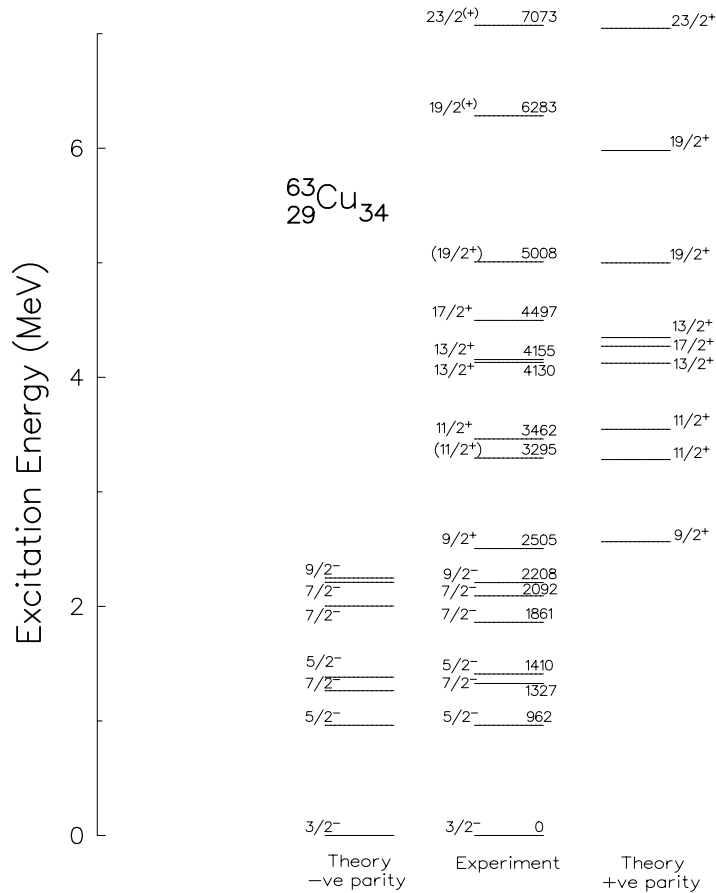


**Figure 4.** A comparison of experimental data and  $fpg$ -shell model calculations for  $^{63}\text{Cu}$ . The highly non-yrast calculated levels are not shown.

$19/2_2^{(+)}$  state at 6283 keV are too low by  $\sim 250$  keV. This may suggest that excitation from the  $f_{7/2}$  orbital in the  $^{56}\text{Ni}$  core is important. However, the high spin states ( $19/2^+$ ) and  $23/2^{(+)}$  are quite well reproduced by this calculation.

### 5. Conclusion

In summary, the high spin states of  $^{63}\text{Cu}$  have been studied with the GDA+CPDA configuration, identifying previously unobserved states up to excitation energy of 7073 keV. This nucleus was populated following the fusion evaporation reaction  $^{52}\text{Cr} + ^{16}\text{O}$ . Detection of evaporated charged particles in CPDA allowed excellent separation of  $\gamma$ -ray transitions associated with the nucleus of interest. From the observed decays of states and DCO ratios, it

was possible to assign spins and parities of many of the states observed. The resulting level scheme has been compared with the shell model calculations using a simple  $fp_g$  basis with no core breaking. In general, reasonable agreement has been established at low excitation energy between experimental results and simple  $fp_g$ -shell model calculations, suggesting that the low-lying yrast excited states in this nucleus correspond predominantly to valence particle excitations into the  $f_{5/2}$ ,  $p_{3/2}$ , and  $p_{1/2}$  orbitals. Higher energy and spin states are fairly well accounted for by allowing only excitations into the +ve parity  $g_{9/2}$  orbital, with no core breaking.

### Acknowledgements

The authors wish to thank the operating crew of the Pelletron facility at Nuclear Science Centre. Special thanks to D Kabiraj of Target Laboratory (NSC) for the help during the target preparation and Prof. N Singh of Punjab University, Chandigarh for allowing us to use the X-ray set-up for the measurement of the target thickness. One of the authors (BM) acknowledges the sincere support and help from S Chanda (VECC, Calcutta) and Dr. S S Ghugre (IUC-DAEF, Calcutta) during the installation period of OXBASH code at NSC. BM also gratefully acknowledges the research grant from the University Grants Commission, India.

### References

- [1] C E Svensson *et al*, *Phys. Rev. Lett.* **79**, 1233 (1997)
- [2] C E Svensson, *Proc. Int. Conf. on Exotic Nuclei and Atomic Masses* (AIP, 1998) p. 407
- [3] M Devlin *et al*, *Phys. Rev. Lett.* **82**, 5217 (1999)
- [4] C E Svensson *et al*, *Phys. Rev. Lett.* **82**, 3400 (1999)
- [5] C H Yu *et al*, *Proc. Int. Conf. on Nuclear Structure* (ORNL, 1998) vol. 1, p. 154
- [6] C E Svensson *et al*, *Phys. Rev. Lett.* **80**, 2558 (1998)
- [7] S D Paul *et al*, *Proc. Int. Conf. on Nuclear Structure* (ORNL, 1998) vol. 1, p. 100
- [8] K P Singh, D C Tayal and H S Hans, *Phys. Rev.* **C58**, 1980 (1998)
- [9] H P L de Esch, J B J M Lanen and C Van Der Leun, *Nucl. Phys.* **A454**, 48 (1986)
- [10] U C Tsan, J F Bruandet, B Chambon, A Dauchy, D Drain, A Giorni, F Glasser and C Morand, *Nucl. Phys.* **A348**, 179 (1980)
- [11] C G Ryan, I Morrison, D L Kennedy, A E Stuchbery and H H Bolotin, *Nucl. Phys.* **A342**, 373 (1980)
- [12] R G Kulkarni *et al*, *Can. J. Phys.* **58**, 472 (1980)
- [13] O M Mustaffa *et al*, *J. Phys.* **G5**, 1283 (1979)
- [14] D Rudolph *et al*, *Phys. Rev. Lett.* **80**, 3018 (1998)
- [15] S C Pancholi and R K Bhowmik, *Indian J. Pure Appl. Phys.* **27**, 660 (1989)
- [16] S Muralithar *et al*, *Proc. DAE Symp. on Nucl. Phys.* **B41**, 404 (1998)
- [17] B Mukherjee, S Muralithar, R P Singh, R Kumar, K Rani and R K Bhowmik, to be published
- [18] A Kramer-Flecken, T Morek, R M Lieder, W Gart, G Hebbinghaus, H M Jager and W Urban, *Nucl. Instrum. Methods* **A275**, 333 (1989)
- [19] B A Brown, A Etchegoyen, W D M Rae and N S Godwin (unpublished)
- [20] J E Koops and P W M Glaudemans, *Z. Phys.* **A280**, 181 (1977)